

Deep-learning-enabled High Electrical-spectral-efficiency Direct Detection with Reduced Computation Complexity

Xingfeng Li¹, Jingchi Li¹, Shaohua An¹, Hudi Liu¹, William Shieh², and Yikai Su^{1,*}

¹State Key Lab of Advanced Optical Communication Systems and Networks, Department of Electronic Engineering, Shanghai Jiao Tong University, Shanghai 200240, China

²School of Engineering, Westlake University, Hangzhou 310030, China

Author e-mail address: yikaisu@sjtu.edu.cn

Abstract: We demonstrate a 50-GBaud complex-valued double-sideband 16-QAM signal transmission over 80-km single-mode fiber with ~64% computational-budget reduction in field reconstruction. This is achieved by using 1×1 convolutions for dimensionality sparsification. © 2023 The Author(s)

1. Introduction

Complex-valued double-sideband (CV-DSB) direct detection (DD) receiver can reconstruct the optical field as a homodyne coherent receiver but without requiring a costly local oscillator laser. Carrier-assisted differential detection (CADD) receiver is a typical CV-DSB DD receiver using delay interferometer structure to reconstruct the optical field [1]. A transmission experiment of a 27-GBaud quadrature phase shift keying (QPSK) signal with a CADD receiver was demonstrated in [2]. Moreover, a silicon photonics (SiP) CADD receiver with a high electrical spectral efficiency (ESE) was also reported [3]. However, a high carrier-to-signal power ratio (CSPR) is required for the CADD receiver, and the receiver structure is complex. In [4], a carrier-less DD receiver with space-time diversity demonstrated the capability of full-field reconstruction based on a chromatic dispersion (CD) element, a delay interferometer structure, and a modified Gerchberg-Saxton (GS) algorithm. Since the signal-to-signal beat interference (SSBI) must be fully detected, the carrier-less DD receiver requires twice receiver electrical bandwidth of that of the homodyne coherent receiver, which leads to a low ESE. In [5], a SiP asymmetric self-coherent detection (ASCD) receiver based on a Mach-Zehnder interferometer was experimentally demonstrated to recover a CV-DSB signal over a 40-km single-mode fiber (SMF). Similar to the CADD receiver, the ASCD receiver also required a high CSPR.

Recently, we have proposed a deep-learning-enabled DD (DLEDD) receiver with dispersion diversity to reconstruct the full field of a CV-DSB signal [6]. We have also demonstrated a transmission experiment of a 42-GBaud 16-ary quadrature amplitude modulation (16-QAM) signal through 80-km SMF with a 5-dB optimum CSPR [7]. Nevertheless, the computational complexity of field reconstruction is the main obstacle to the application of the DLEDD scheme. In this paper, we use 1×1 convolutions to realize a sparse dimensionality (in particular the number of channels) of the deep convolutional neural network (CNN). Compared with our previous work, the proposed scheme can reduce the real-valued multiplications per symbol by ~64% without performance degradation. As a proof-of-concept experiment, we demonstrate a 50-GBaud 16-QAM signal transmission over 80-km SMF with a 5-dB optimum CSPR. Considering the frame redundancy and 25% forward error correction (FEC) overhead, we achieve a net data rate of 159.2 Gb/s and a high ESE on one polarization of 5.69 b/s/Hz.

2. Operation principle

Fig. 1(a) illustrates the schematic of the deep CNN structure in the DLEDD. The deep CNN consists of three stacked residual blocks. Each residual block contains two convolutional layers. The kernel sizes of the six convolutional layers are 13. The featured channel numbers of the convolutional layer are also larger than 30. Large kernel size and featured channel number results in an expensive computational budget for implementing a convolutional layer. For example, 10880 real-valued multiplications per symbol are required for the first convolutional layer in the first residual block, as shown in Fig. 1(b). Here, n represents the sequence length. In our proposed scheme, a 1×1 convolutional layer is inserted before the convolutional layer with a large kernel size to reduce the required real-valued multiplications, since 1×1 convolution has a powerful ability in dimensionality sparsification [8]. The output channel number of the 1×1 convolutional layer is set to 10. By employing a 1×1 convolutional layer, the required real-valued multiplications per symbol is reduced to 4740. In our previous work, $\sim 10^5$ real-valued multiplications are required to reconstruct the field of one symbol. In this work, if the proposed convolutional method is used for all the six convolutional layers of the three residual blocks, only $\sim 3.6\times 10^4$ real-valued multiplications are required after dimensionality sparsification. Thus, the computational complexity of the field reconstruction is decreased by ~64%.

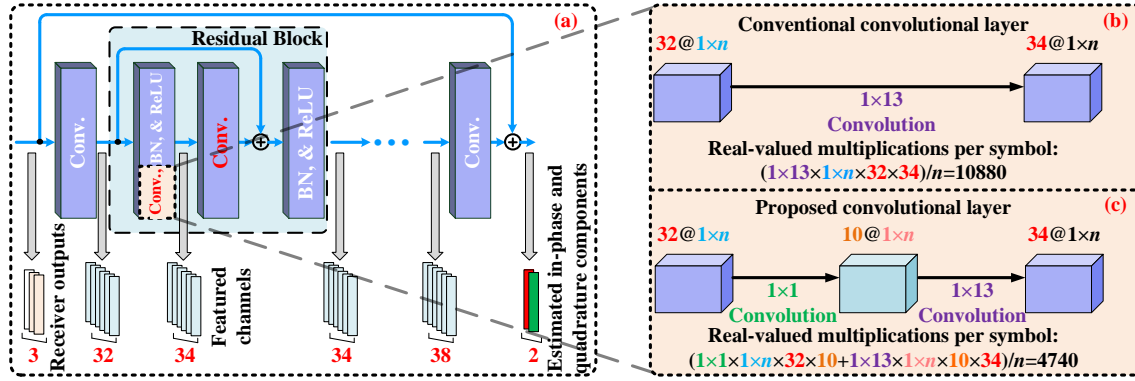


Fig. 1. (a) Schematic of the deep CNN structure in the DLEDD. Zoom-in of the (b) conventional and (c) proposed convolutional layer.

3. Experimental setup and results

Fig. 2(a) shows the experimental setup. A 100-GSa/s digital-to-analog converter (DAC) (MICRAM DAC10002) generates a 50-Gbaud dual-SSB 16-QAM signal with a 6-GHz guard band between upper and lower sidebands. After being amplified by two electrical amplifiers (EAs), the dual-SSB 16-QAM signal drives a 35-GHz in-phase and quadrature modulator (IQM) biased at its transmission null. A continuous-wave light from an external cavity laser (ECL) at 1550 nm is split into two branches for inputting the IQM and providing a carrier. We use a polarizer to align the polarization states of both the 16-QAM signal and the carrier. A variable optical attenuator (VOA) is employed to adjust the CSRR of the CV-DSB signal. Before launched into an 80-km SMF, the CV-DSB signal is boosted by an erbium-doped fiber amplifier (EDFA). At the receiver side, the dispersion values of the two dispersion compensation modules (DCMs) are -134.4 , and -1008 ps/nm, respectively. Finally, the electrical signals are sampled by an 80-GSa/s digital storage oscilloscope (DSO) (LeCroy 36Zi-A). The digital signal processing (DSP) flow charts are presented in Fig. 2(b). Deep CNN is used to reconstruct the field of the CV-DSB signal. 1×1 convolution is employed to reduce the computational complexity of convolutional layer in residual block. Fig. 2(c) presents the optical spectra measured at different stages.

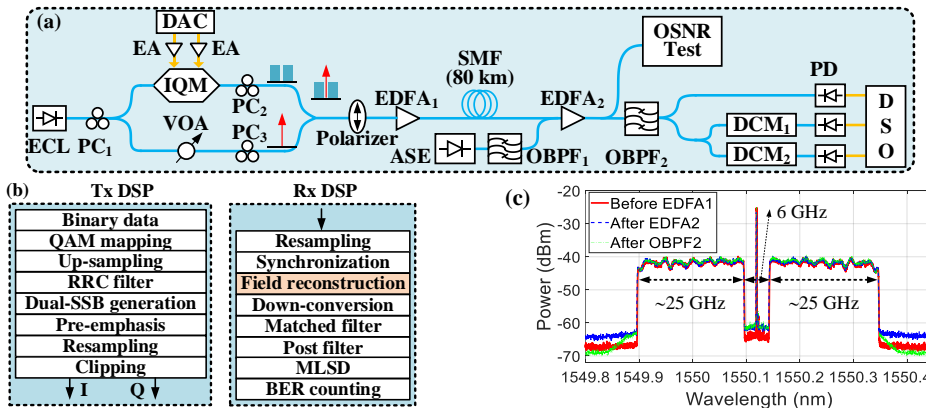


Fig. 2. (a) Experimental setup. (b) DSP flow charts. (c) Optical spectra measured at different stages. ASE: amplified spontaneous emission; BER: bit error ratio; MLSD: maximum likelihood sequence detection; OBPF: optical band-pass filter; OSNR: optical signal-to-noise ratio; PC: polarization controller; PD: photodiode; RRC filter: root raised cosine filter.

Fig. 3(a) shows the BER versus CSRR for different OSNRs. Compared with the conventional convolutional scheme without 1×1 convolutions, the proposed convolutional scheme performs better. This can be attributed to two factors: 1) the reduced redundancy information of the CNN via dimensionality sparsification; 2) the increased depth of the CNN [8]. Moreover, the CNN has a more powerful capability for nonlinear modeling. At the 25-dB OSNR, the optimum CSRR is ~ 5 dB for both the optical back-to-back (OBTB) and the 80-km transmission cases. Fig. 3(b) shows the BER versus OSNR for different CSRRs. The results about the optimum CSRR shown in Fig. 3(b) are consistent with that in Fig. 3(a). Fig. 3(c) presents the BER versus OSNR for different output channel numbers of the 1×1 convolutional layers. At a low OSNR value, the BER is limited by the noise instead of SSBI. Thus, the BER is insensitive to the CNN structure. The BER curves nearly overlap. As the OSNR increases, the BER curves gradually diverge. That is because that the BER is mainly limited by the SSBI. Thus, it becomes more sensitive to the CNN structure. Moreover, the more featured channels the CNN comprises, the stronger SSBI mitigation ability it has. Considering the trade-off between the performance and complexity, we select 10 as the output channel numbers.

For the OBTB and 80-km transmission cases with or without 1×1 convolutions in Fig. 3(a), the constellations of the recovered 16-QAM signals at different OSNR and CSNR are also provided in the insets. Table 1 compares the experimental results of various CV-DSB DD schemes. Compared with our previous work, the proposed scheme can reduce the real-valued multiplications per symbol by $\sim 64\%$ without performance degradation.

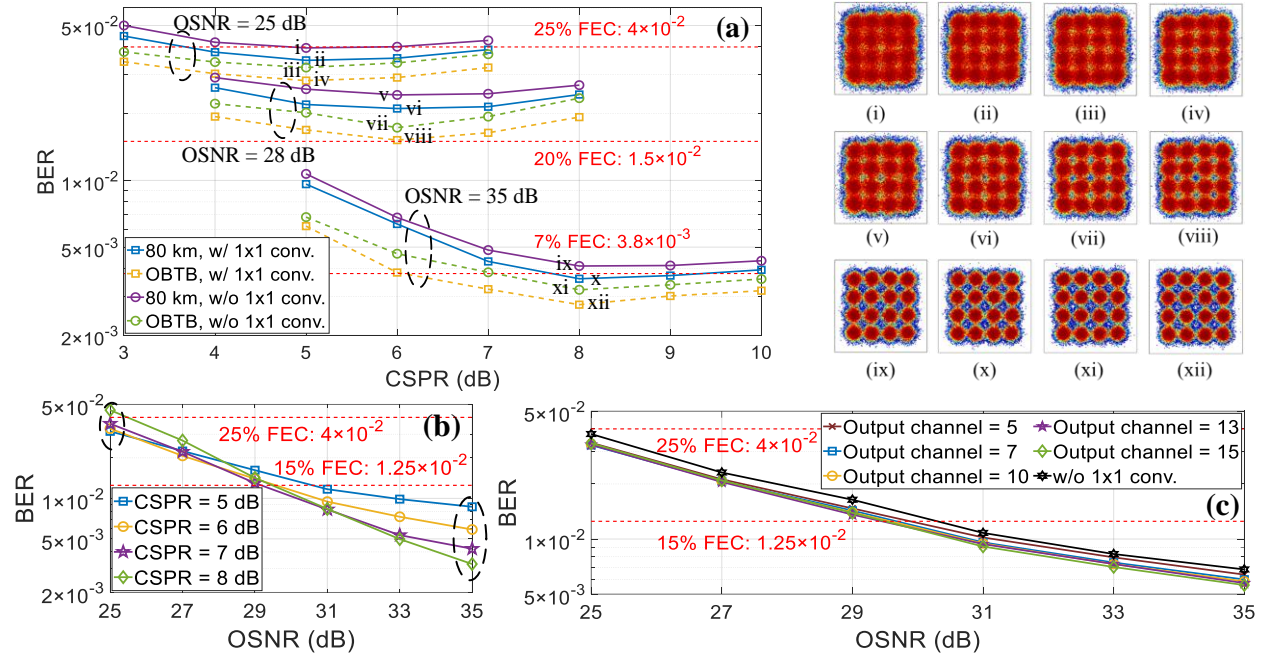


Fig. 3. (a) BER versus CSNR for different OSNRs. (b) BER versus OSNR for different CSNRs. (c) BER versus OSNR for different output channel numbers of 1×1 convolutional layers at 6-dB CSNR. Insets (i-iv): constellations at 25-dB OSNR and 5-dB CSNR; insets (v-viii): constellations at 28-dB OSNR and 6-dB CSNR; insets (ix-xii): constellations at 35-dB OSNR and 8-dB CSNR.

Table 1. Comparisons of CV-DSB DD schemes

Detection schemes	Baud rate (GBaud)	Modulation format	Net rate (Gb/s)	Receiver bandwidth (GHz)	ESE per polarization (b/s/Hz)	Transmission distance (km)	Optimum CSNR (dB)	Real-valued multiplications per symbol
GS [4]	40	16-QAM	140	80	1.75	40	$-\infty$	$\sim 10^4$
CADD [2]	27	QPSK	<50.5	15.93	<3.17	160	7	$\sim 10^3$
SiP CADD [3]	56	16-QAM	162	35	4.63	80	12	$\sim 10^3$
SiP ASCD [5]	60	16-QAM	200	34	5.86	40	15	$\sim 10^3$
DLEDD [7]	42	16-QAM	133.7	24	5.57	80	5	$\sim 10^5$
This work	50	16-QAM	159.2	28	5.69	80	5	$\sim 3.6 \times 10^4$

4. Conclusion

In this paper, we used 1×1 convolutions to realize a sparse dimensionality of the CNN in the DLEDD system. Compared with our previous work, the proposed scheme can reduce the computational complexity of the field reconstruction by $\sim 64\%$ without performance degradation. We demonstrated a 50-GBaud 16-QAM signal transmission over 80-km SMF with a 5-dB optimum CSNR and a 5.69-b/s/Hz ESE.

5. References

- [1] W. Shieh *et al.*, "Carrier-assisted differential detection," *Light-Sci. Appl.* **9**, 1-9 (2020).
- [2] C. Sun *et al.*, "Experimental Demonstration of Complex-valued DSB Signal Field Recovery via Direct Detection," *IEEE Photon. Tech. L.* **32**, 585-588 (2020).
- [3] J. Li *et al.*, "High Electrical Spectral Efficiency Silicon Photonic Receiver with Carrier-Assisted Differential Detection," in *Proc. OFC, Post-deadline Paper Th4B.6*, (2022).
- [4] H. Chen *et al.*, "140G/70G Direct Detection PON with >37 dB Power Budget and 40-km Reach Enabled by Colorless Phase Retrieval Full Field Recovery," in *Proc. ECOC, Post-deadline Paper Th3C.1*, (2021).
- [5] Y. Hu *et al.*, "Transmission of Net 200 Gbps/λ over 40 km of SMF Using an Integrated SiP Phase-Diverse Receiver," in *Proc. ECOC, Post-deadline Paper Th3B.6*, (2022).
- [6] X. Li *et al.*, "Deep-Learning-Enabled High-Performance Full-Field Direct Detection with Dispersion Diversity," *Opt. Express* **30**, 11767-11788 (2022).
- [7] X. Li *et al.*, "Deep-learning Enabled Direct Detection of 42-GBaud Complex-valued DSB 16-QAM Signal," in *Proc. CLEO, SW4E.4*, (2022).
- [8] C. Szegedy *et al.*, "Going Deeper with Convolutions," in *Proc. CVPR*, 1-9, (2015).